Acceleron Aerospace Journal || AAJ.11.2106-2464
Volume 3, Issue 6, pp (624-647)
Research Paper
E-ISSN- 2583-9942 || DOI: 10.61359/11.2106-2464

Sharp Cone-Broad Cone-Disk: Analytical Solutions in the Tunnel Mathematics Space to the Steady Navier-Stokes Equations in the Area of Boundary Layer for Incompressible Symmetric Flows Entrained by these Rotating Bodies

Oleh G. Shvydkyi *

Independent Researcher, Zaporizhzhia, Ukraine

Abstract: More than 150 years of history of efforts to solve the Navier-Stokes equation have clearly shown that, applying standard mathematical tools, it is possible to do this in only a small number of simple cases. Therefore, to solve such equations, we can try non-standard methods of mathematical modeling. In this case, the emphasis should be placed not on the mathematical accuracy of the proposed solutions, but on their correspondence to experimental data or solutions to the Navier-Stokes equations obtained by numerical methods. We believe that tunnel mathematics is such a method of mathematical modeling. Main theorem of tunnel mathematics allows us to reduce a system of the steady Navier-Stokes equations to simple ordinary differential equations that give solutions in planes parallel to the basic *xy* plane. Collecting such solutions, we finally obtain full 3D solution of a system of the steady Navier-Stokes equations. Approximate solutions for a system Sharp cone—Broad cone—Disk in the area of boundary layer can be obtained without use of specific software (including case of turbulent motion of fluid). We get solution for a rotating disk as a limit transition for a broad cone. If such solution will be similar with famous Karman`s solution for a rotating disk (we mean laminar flows), then we could conclude that our theory is successive.

Table of Contents

1. Introduction

Despite the widespread use of numerical methods for solving Navier-Stokes equations some researchers actively develop analytical ones. For example, Jaroslav Štigler obtained analytical formula for velocity distribution law in fluids moving in pipes [3]; Bo Zhao et al. solved analytically Navier-Stokes equations for unsteady flow entrained by rotating disk for low Reynolds numbers [4]; Biruk Alemayehu Petros solve Navier-Stokes equations for incompressible fluids via local linearization of variable functions [5]; Taofiq O. Amoloye fulfilled analysis of an unsteady incompressible crossflow on a stationary circular cylinder using refined potential flow theory [13]. The nature of flows over rotating disks and cones is shown very well in papers by P. Henrik Alfredsson et al. [6] and Kentaro KATO et al. [14]. In these papers the steady Navier-Stokes equations in the laboratory frame of reference are transformed into set of ordinary differential equations (Karman`s solution). Also, theoretical aspects of flow over rotating disk study can be found in treatises by Landau [1] and Schlichting [2].
System Sharp cone—Broad cone—Disk is shown in Figure. 1. Flows over rotating disk and broad cone are similar due to large influence of centrifugal forces.

*Research Scholar, Independent Researcher, Zaporizhzhia, Ukraine. **Corresponding Author: oleg.shv.jw@gmail.com**
** Received: 20-November-2024 || Revised: 26-November-2024 || Accepted: 28-November-2024 || Published Online: 30-November-2024.

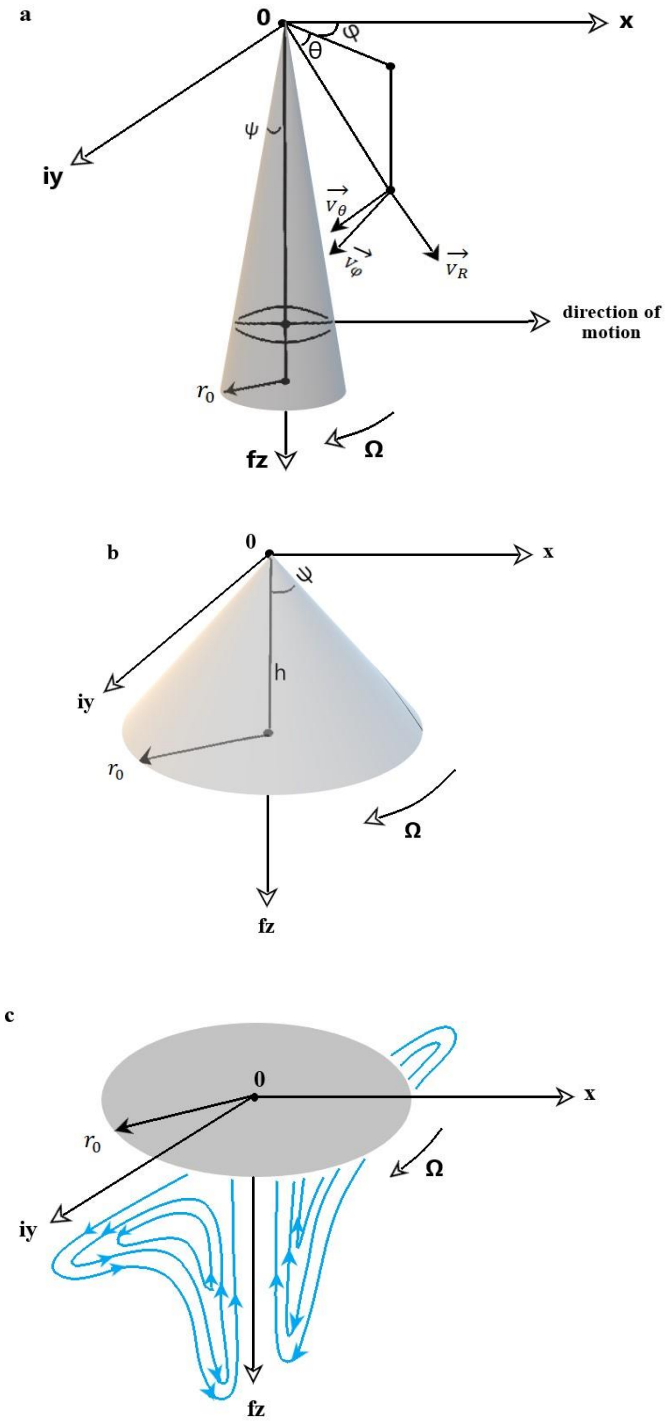

Figure-1. (a) Sharp cone: ψ — half-apex angle of cone, φ — azimuthal angle, θ — polar angle, V_R, V_θ, V_φ— velocity field components in modified spherical system of coordinates (*we measure polar angle θ from xy plane, not from z axis, as usually*), r_0— cone base and disk radius, Ω — angular velocity of rotation; the arrow indicates the direction of movement in the plane where the pressure is calculated. (b) Broad cone: h — cone height. (c) Disk: sketch of laminar flows under rotating disk in the laboratory frame.

Since the time of Laplace, integral transforms have been used to solve partial differential equations (PDE). Today many integral transform exist although they differ from Laplace transform insignificantly. Especially integral transforms are helpful to solve PDE with constant coefficients [7, 8]. Also, some of them can

be successively applied to solve nonlinear PDE, however the number of terms in such equations remains as a rule small (about four **[9]**). This significantly complicates the use of integral transform to solve nonlinear Navier-Stokes equations where only laplacians of velocity field components in spherical system of coordinates have at least five terms (almost all with variable coefficients, see (26) – (32)).

Against this background, the use of tunnel mathematics can become an effective tool for solving nonlinear Navier-Stokes equations. Tunnel mathematics is a type of mathematical modeling when, according to certain laws and boundary conditions, we create components of the velocity field in a fluid. Of course, these created components are not the exact solutions of Navier-Stokes equations. However, adjusting the calibration coefficients we can fit them to as more as possible satisfy to experimental data. Main theorem of tunnel mathematics allows us to compute a pressure distribution field of incompressible fluid in the planes parallel to the basic *xy* plane (i.e. in the planes $z = const$, so-called *working platforms*) **[11]**. Comparing obtained results with experimental data (such data already exist, for example, for certain configurations of Broad cone — Disk system **[10]**), we can estimate an accuracy of our modeling.

Besides, use of tunnel mathematics has certain advantages because it allows to work with laplacians of functions very easily. For instance, following relations hold in tunnel mathematics:

$$P = u(x,y,z) + iv(x,y,z) + fw(x,y,z); \tag{1}$$

where P is a spatial function of complex variable; functions u, v and w are the functions of real variables x, y, z; f is a special operator of tunnel mathematics.

$$\Delta u = 0; \tag{2}$$
$$\Delta v = 0; \tag{3}$$

Relations (2) and (3) are ordinary ones for planar theory of complex variable **[7, 11]**.

$$\Delta(uw) = \frac{(vw)x}{y^3} - \frac{(y^2-x^2)}{xy}C_i - C_r; \tag{4}$$

$$\Delta(vw) = \frac{(uw)y}{x^3} - \frac{(y^2-x^2)}{xy}C_r + C_i; \tag{5}$$

where constants C_r and C_i, which can to depend on z coordinate, are included in the following relations:

$$\frac{\partial(uw)}{\partial x} + i\frac{\partial(uw)}{\partial y} = (C_r + iC_i)x; \tag{6}$$

$$\frac{\partial(vw)}{\partial x} + i\frac{\partial(vw)}{\partial y} = -(C_r + iC_i)y. \tag{7}$$

In (2) – (5) $\Delta = \frac{\partial^2}{\partial x^2} + \frac{\partial^2}{\partial y^2}$ is the Laplace operator on the *xy* plane (on the working platforms).
Relations (4) and (5) shows that on the working platforms Laplacians of functions linearly depend from the functions themselves which essentially simplifies the solution of differential equations. And since Laplacians are included in a large number of physical equations (for example, in the Schrodinger equation in quantum mechanics, the Lame equation in theory of elasticity, the eikonal equation in optics, etc.) it seems that tunnel mathematics has every chance taking its rightful place in theoretical physics.

2. Theory

Theoretical Overview. We work in modified spherical system of coordinates; i.e. *we measure polar angle θ from xy plane (not from z axis, as usually)* (Fig. 1). So, we need carry out following transformation with ordinary spherical system of coordinates:

$$v_\theta \to -v_\theta;$$
$$\theta \to \frac{\pi}{2} - \theta; \tag{8}$$
$$\partial\theta \to -\partial\theta.$$

2.1. Main equations of tunnel mathematics

Tunnel mathematics equations applied to the components of the vector velocity field in Cartesian coordinate system look like this **[11]**:

$$\frac{\partial u}{\partial x} + \frac{(uw)y}{(x^2+y^2)^{3/2}}\left(2+\left(\frac{y}{x}\right)^2\right) + \frac{1}{\sqrt{x^2+y^2}}\frac{\partial(vw)}{\partial x} = \frac{\partial v}{\partial y} - \frac{(vw)x}{(x^2+y^2)^{3/2}}\left(2+\left(\frac{x}{y}\right)^2\right) - \frac{1}{\sqrt{x^2+y^2}}\frac{\partial(uw)}{\partial y} = -\frac{2y}{\sqrt{x^2+y^2}}\frac{\partial u}{\partial z} + \frac{1}{x}\cdot\frac{\partial(uw)}{\partial z} + \frac{1}{y}\cdot\frac{\partial(vw)}{\partial z} - \frac{2y}{(x^2+y^2)}\frac{\partial(vw)}{\partial z}; \tag{9}$$

$$\frac{\partial v}{\partial x} + \frac{(vw)y}{(x^2+y^2)^{3/2}} - \frac{1}{\sqrt{x^2+y^2}}\frac{\partial(uw)}{\partial x} = -\frac{\partial u}{\partial y} + \frac{(uw)x}{(x^2+y^2)^{3/2}} - \frac{1}{\sqrt{x^2+y^2}}\frac{\partial(vw)}{\partial y} = -\frac{2y}{\sqrt{x^2+y^2}}\frac{\partial v}{\partial z} + \frac{2y}{(x^2+y^2)}\frac{\partial(uw)}{\partial z}; \tag{10}$$

$$\frac{1}{x}\cdot\frac{\partial(uw)}{\partial x} + \frac{1}{y}\cdot\frac{\partial(vw)}{\partial x} = -\frac{i}{y}\cdot\frac{\partial(vw)}{\partial y} - \frac{i}{x}\cdot\frac{\partial(uw)}{\partial y} = -\frac{\partial u}{\partial z} - i\frac{\partial v}{\partial z} + \frac{i}{\sqrt{x^2+y^2}}\cdot\frac{\partial(uw)}{\partial z} - \frac{1}{\sqrt{x^2+y^2}}\cdot\frac{\partial(vw)}{\partial z}. \tag{11}$$

Equations (9) and (10) have algebraic nature; equation (11) has *complex nature*. It is easy seen that at $w = 0$ equations (9) and (10) transform into ordinary planar Cauchy-Riemann conditions **[7, 11]**; and equation (11) disappears.

Functions *u*, *v*, *w* in (1) – (7), (9) – (11) correspond to the vector velocity field components in Cartesian coordinate system. So, such relations connect the vector velocity field components in Cartesian and modified (8) spherical coordinate systems:

$$u = v_x = \cos\varphi\,(v_R\cos\theta - v_\theta\sin\theta) - v_\varphi\sin\varphi\,; \tag{12}$$

$$v = v_y = \sin\varphi\,(v_R\cos\theta - v_\theta\sin\theta) + v_\varphi\cos\varphi\,; \tag{13}$$

$$w = v_z = v_R\sin\theta + v_\theta\cos\theta\,; \tag{14}$$

There are also inverse transition formulas:

$$v_R = \cos\theta\,(u\cos\varphi + v\sin\varphi) + w\sin\theta\,; \tag{15}$$

$$v_\theta = -\sin\theta\,(u\cos\varphi + v\sin\varphi) + w\cos\theta\,; \tag{16}$$

$$v_\varphi = -u\sin\varphi + v\cos\varphi\,; \tag{17}$$

and ordinary transition formulas between Cartesian and modified (8) spherical coordinate systems hold:

$$x = R\cos\theta\cos\varphi\,; \tag{18}$$

$$y = R\cos\theta\sin\varphi\,; \tag{19}$$

$$z = R\sin\theta. \tag{20}$$

Recall that we work in modified (8) spherical system of coordinates; i.e. *we measure polar angle θ from xy plane (not from z axis as usually)* (Fig. 1).

Using (12) – (14) we arrive to the following relations:

$$(uw) = \cos\varphi\left((v_R^2 - v_\theta^2)\frac{\sin 2\theta}{2} + v_R v_\theta\cos 2\theta\right) - v_\varphi\sin\varphi\,(v_R\sin\theta + v_\theta\cos\theta); \tag{21}$$

$$(vw) = \sin\varphi\left((v_R^2 - v_\theta^2)\frac{\sin 2\theta}{2} + v_R v_\theta\cos 2\theta\right) + v_\varphi\cos\varphi\,(v_R\sin\theta + v_\theta\cos\theta); \tag{22}$$

For our Sharp cone — Broad cone — Disk system we will consider two limit case:

1. Sharp cone: $v_R, v_\theta \gg v_\varphi$ (large streamwise flows). So, taking into account (18) and (19) we can obtain from (21) and (22) such simple condition for sharp cone:

$$(uw)y = (vw)x. \tag{23}$$

2. Broad cone: $v_R, v_\theta \ll v_\varphi$ (large centrifugal flows). In the same way as the condition for a sharp cone was obtained, we arrive at the condition for a broad cone:

$$(uw)x = -(vw)y. \tag{24}$$

We will get solution for a rotating disk as a limit transition for a broad cone.

3. Steady Navier-Stokes equations

In general tensor form the steady Navier-Stokes equations are represented as follows [12]:

$$\rho v_k\frac{\partial v_i}{\partial x_k} = -\frac{\partial P}{\partial x_i} + \mu\left(\frac{\partial^2 v_i}{\partial x_k\partial x_k} + \frac{1}{3}\frac{\partial}{\partial x_i}\left(\frac{\partial v_l}{\partial x_l}\right)\right) + \left(\frac{\partial v_i}{\partial x_k} + \frac{\partial v_k}{\partial x_i} - \frac{2}{3}\delta_{ik}\frac{\partial v_l}{\partial x_l}\right)\times\left(\frac{\partial\mu}{\partial x_k}\right); \tag{25}$$

where δ_{ik} is the Kronecker symbol: $\delta_{ik} = \begin{cases}1, if\ i = k;\\ 0, if\ i \neq k;\end{cases}$

besides,

ρ is a density of fluid;
v_i is a *ith* component of vector velocity field;
P is a pressure in fluid;
μ is a dynamic viscosity of fluid.

Last term in (25) represent a tensor product.

For incompressible case the term corresponding to divergence of vector velocity field in (25) is zero; the dynamic viscosity μ is constant and last term is zero as well.

So, Navier-Stokes equations (25) in modified (8) spherical polar coordinates assume such form for incompressible case:

$$\rho\left(v_R\frac{\partial v_R}{\partial R}+v_\theta\frac{\partial v_R}{R\partial\theta}-\frac{(v_\theta^2+v_\varphi^2)}{R}\right)=-\frac{\partial P}{\partial R}+\mu\left(\Delta v_R-\frac{2v_R}{R^2}-\frac{2}{R^2}\frac{\partial v_\theta}{\partial\theta}+\frac{2v_\theta}{R^2}\tan\theta\right); \quad (26)$$

$$\rho\left(v_R\frac{\partial v_\theta}{\partial R}+v_\theta\frac{\partial v_\theta}{R\partial\theta}+\frac{v_Rv_\theta}{R}+\frac{v_\varphi^2\tan\theta}{R}\right)=-\frac{\partial P}{R\partial\theta}-\mu\left(\Delta v_\theta-\frac{2}{R^2}\frac{\partial v_R}{\partial\theta}+\frac{v_\theta}{(R\cos\theta)^2}\right); \quad (27)$$

$$\rho\left(v_R\frac{\partial v_\varphi}{\partial R}+v_\theta\frac{\partial v_\varphi}{R\partial\theta}+\frac{v_Rv_\varphi}{R}-\frac{v_\theta v_\varphi\tan\theta}{R}\right)=\mu\left(\Delta v_\varphi-\frac{v_\varphi}{(R\cos\theta)^2}\right); \quad (28)$$

$$\frac{\partial v_R}{\partial R}+\frac{2v_R}{R}+\frac{\partial v_\theta}{R\partial\theta}-\frac{v_\theta\tan\theta}{R}=0; \quad (29)$$

where

$$\Delta v_R=\frac{\partial^2 v_R}{\partial R^2}+\frac{2}{R}\frac{\partial v_R}{\partial R}+\frac{1}{R^2}\frac{\partial^2 v_R}{\partial\theta^2}-\frac{\tan\theta}{R^2}\frac{\partial v_R}{\partial\theta}; \quad (30)$$

$$\Delta v_\theta=-\frac{\partial^2 v_\theta}{\partial R^2}-\frac{2}{R}\frac{\partial v_\theta}{\partial R}-\frac{1}{R^2}\frac{\partial^2 v_\theta}{\partial\theta^2}+\frac{\tan\theta}{R^2}\frac{\partial v_\theta}{\partial\theta}; \quad (31)$$

$$\Delta v_\varphi=\frac{\partial^2 v_\varphi}{\partial R^2}+\frac{2}{R}\frac{\partial v_\varphi}{\partial R}+\frac{1}{R^2}\frac{\partial^2 v_\varphi}{\partial\theta^2}-\frac{\tan\theta}{R^2}\frac{\partial v_\varphi}{\partial\theta}. \quad (32)$$

Equations (26) – (28) are written without taking into account gravitational force; so, the pressure P in that equations is a difference between actual pressure in some point and hydrostatic pressure in the same point.

Flows over Sharp cone — Broad cone — Disk system are axisymmetric that is why in (26) – (32) all derivatives by the azimuthal angle φ are zero.

Relation (29) represent the equation of continuity for incompressible case.

4. Result and Discussion

4.1 Sharp cone

4.1.1 Finding velocity components

$$(uw) = \frac{A_0^2 b^2 a}{y(x^2+y^2)} \exp\left[z\sqrt{x^2+y^2}\left(\frac{4xy}{(x^2+y^2)^2}+\frac{1}{xy}\right)\right]; \tag{33}$$

$$(vw) = \frac{A_0^2 b^2 a}{x(x^2+y^2)} \exp\left[z\sqrt{x^2+y^2}\left(\frac{4xy}{(x^2+y^2)^2}+\frac{1}{xy}\right)\right]; \tag{34}$$

where A_0, a, b are the constants; $[A_0] = \frac{m}{sec}$; $[a] = [b] = m$.

Now we can construct the components of the vector velocity field in Cartesian coordinate system. In order to satisfy (23) we select the components of analytical functions [7] in following manner:

$$u = A_0 \frac{x}{a}; \tag{35}$$

$$v = A_0 \frac{y}{a}. \tag{36}$$

It is easy seen that (2) and (3) are satisfied automatically. Then we obtain from (33) and (34) such relation for w:

$$w = A_0 \frac{(ab)^2}{xy(x^2+y^2)} \exp\left[z\sqrt{x^2+y^2}\left(\frac{4xy}{(x^2+y^2)^2}+\frac{1}{xy}\right)\right]; \tag{37}$$

Now using (15), (16), (18) – (20) we can obtain the components of the vector velocity field in modified (8) spherical coordinate system:

$$v_R = A_0\left(\frac{(R\cos\theta)}{a}\cos\theta + \sin\theta\frac{2(ab)^2}{A_2(R\cos\theta)^4}\exp[2A_1\,tan\,\theta]\right); \tag{38}$$

$$v_\theta = A_0\left(-\frac{(R\cos\theta)}{a}\sin\theta + \cos\theta\frac{2(ab)^2}{A_2(R\cos\theta)^4}\exp[2A_1\,tan\,\theta]\right); \tag{39}$$

where $A_1\ and\ A_2$ are dimensionless constants (they depend on φ).

We seek the solutions of Navier-Stokes equations in the area of boundary layer, that is why we need to impose the so called non-slip boundary conditions on (38) and (39):

$$\text{at } \theta = \theta_w = \frac{\pi}{2} - \psi \text{ should be } v_R = 0 \text{ and } v_\theta = 0; \tag{40}$$

where ψ is the half-apex angle of cone (Fig. 1).

In order to satisfy (40) the relations (38) and (39) must take such form:

$$v_R = A_0\left(\frac{(R\cos\theta)}{a}\cos\theta + \frac{\sin\theta}{(\cos\theta)^4}\frac{\gamma_2'}{R^4}\left(\frac{R^5\delta_2'}{tan\,\theta_w}\right)^\alpha\cos\pi\alpha\right); \tag{41}$$

$$v_\theta = A_0\left(-\frac{(R\cos\theta)}{a}\sin\theta + \frac{\cos\theta}{(\cos\theta)^4}\frac{\gamma_2'}{R^4}(R^5\delta_2'\,tan\,\theta_w)^\alpha\right); \tag{42}$$

where

$$\alpha = \frac{tan\,\theta}{tan\,\theta_w}; \tag{43}$$

$$\gamma_2' = \frac{2(ab)^2}{A_2};\ [\gamma_2'] = m^4; \tag{44}$$

$$\delta_2' = \frac{A_2(\cos\theta_w)^5}{2(ab)^2 a};\ [\delta_2'] = m^{-5}; \tag{45}$$

we keep the notations adopted in **[12]**.

Using (17) – (19) and (35), (36) we arrive to such expression for v_φ component:

$$v_\varphi = -u\sin\varphi + v\cos\varphi = 0. \tag{46}$$

In other words, our model for a sharp cone assumes that the cone itself is at rest under the incident flow; i.e. we seem to be moving into a reference system coupled with a cone, while neglecting centrifugal forces (which is permissible for a sharp cone).

In the Figs. 2 and 3 below the graphs for v_R and v_θ components corresponding to (41) and (42) are shown.

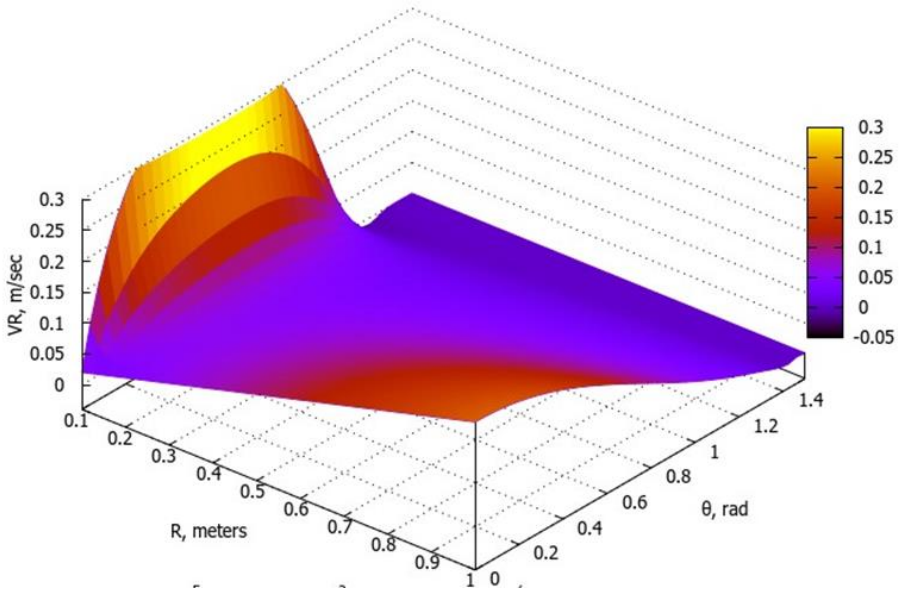

Figure-2. Graph for v_R component in (41) at $\psi = 10°$ ($\theta_w = 80°$ ($1.4\ rad$)) and $A_0 = 200\ \frac{m}{sec}$.

When constructing graphs in Figs. 2 and 3, we assume the values of the remaining constants as follows:

$$a = 1000\ m; \tag{47}$$

$$b = 0.001\ m; \tag{48}$$

$$A_2 = 2 \cdot 10^6. \tag{49}$$

What is striking in the figures is the step-by-step change in both components of velocity (similar to a quantum change) as you approach the apex of the cone.

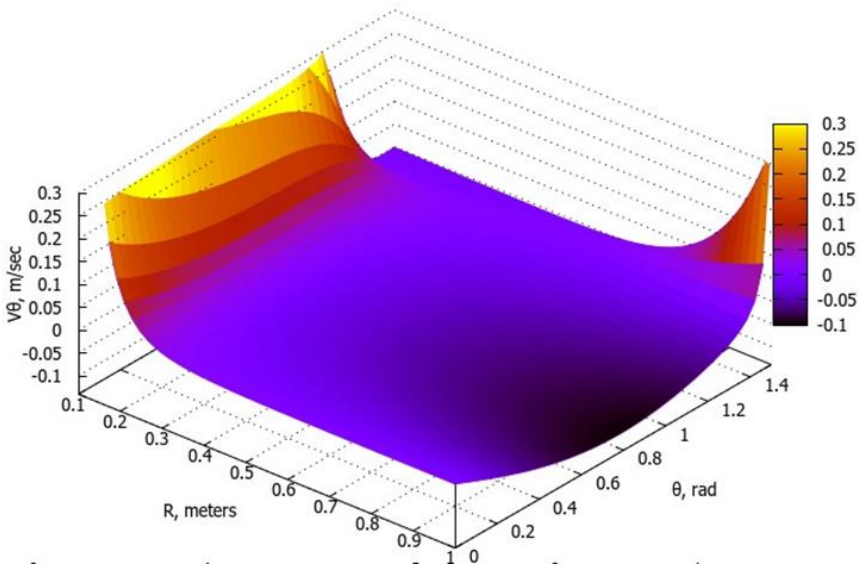

Figure-3. Graph for v_θ component in (42) at $\psi = 10°$ ($\theta_w = 80°$ ($1.4\ rad$)) and $A_0 = 200\ \frac{m}{sec}$.

4.1.2 Finding pressure

Now we can check the equation of continuity for incompressible case. Substituting (41) and (42) in (29), we obtain such expression:

$$\frac{\partial v_R}{\partial R} + \frac{2v_R}{R} + \frac{\partial v_\theta}{R\partial\theta} - \frac{v_\theta \tan\theta}{R} = A_0\left(\frac{2}{a} + R^{5(\alpha-1)}\frac{\sin\theta}{(\cos\theta)^4}\gamma_2'(\delta_2'\,(tan\,\theta_w)^{-2})^\alpha\beta\right); \quad (50)$$

where

$$\beta = (5\alpha - 2)\cos\pi\alpha + 2\,(tan\,\theta_w)^{2\alpha}\,; \quad (51)$$

Below in Fig. 4 the graph for β is shown.

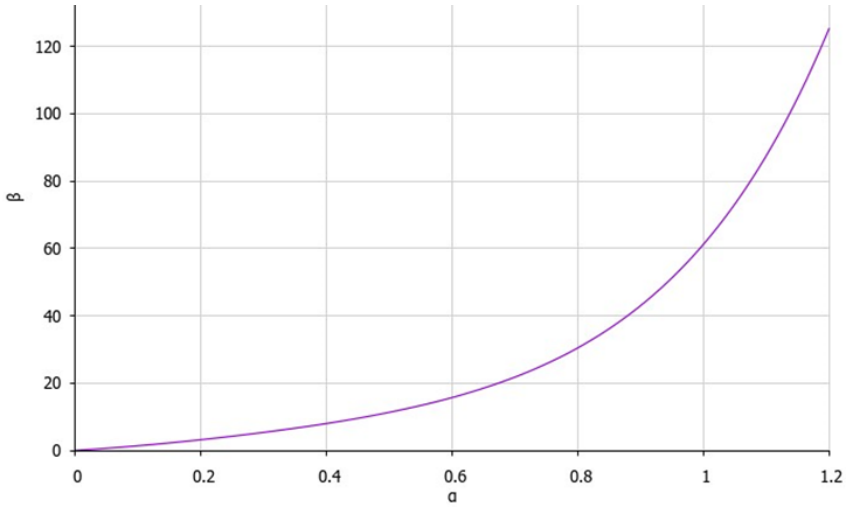

Figure-4. The graph for β in (51). The area of boundary layer is near $\alpha = 1$.

By giving constants values indicated in (47) – (49) we can ensure that the expression (50) does not exceed the values of v_R and v_θ.

Now we consider the following combination of components (41) and (42):

$$v_R \tan\theta + v_\theta = A_0 \frac{\gamma_2'}{(R\cos\theta)^4} (R^5\delta_2')^\alpha (\tan\theta_w)^{-\alpha}\beta_1; \quad (52)$$

where

$$\beta_1 = \frac{\sin^2\theta}{\cos\theta}\cos\pi\alpha + \cos\theta\,(\tan\theta_w)^{2\alpha}; \quad (53)$$

Below in Fig. 5 the graph for β_1 is shown.

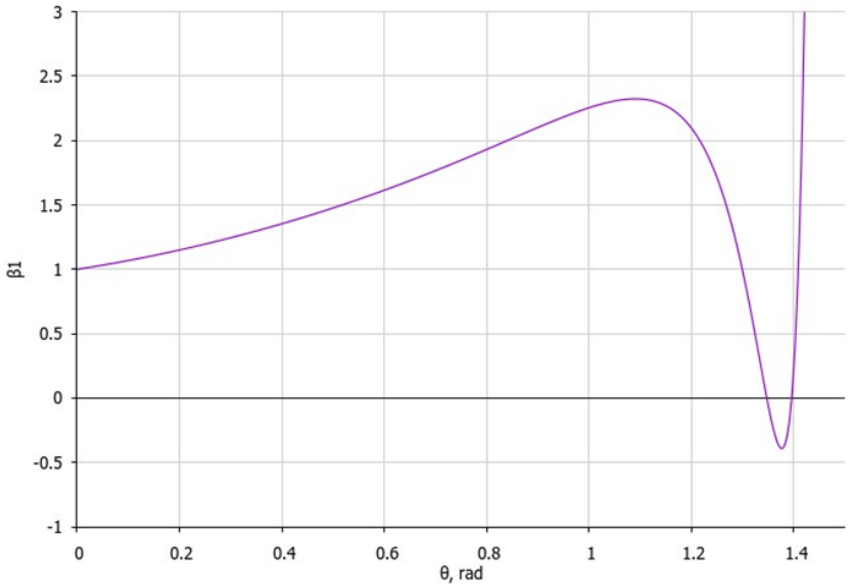

Figure-5. The graph for β_1 in (53). The area of boundary layer is near $\theta \approx 1.4$.

It is seen from Fig. 5 that we can assume that the expression $v_R \tan\theta + v_\theta$ in (52) and its first and second derivatives are approximately equal to zero in the area of boundary layer ($\theta \approx 1.4$).

This will allow us to significantly simplify the solution of the Navier-Stokes equations in the area of boundary layer.

Now we translate the Navier-Stokes equations (26) and (27) into the plane

$$z = R\sin\theta = const = 0.5. \quad (54)$$

Numerical results for solving the Navier-Stokes equations in the plane exist in the literature **[15]**.

Equation (28) for our model of sharp cone disappears due to (46).

The following relation applies in the plane (54):

$$\frac{dR}{d\theta} = -R\cot\theta. \quad (55)$$

We use (55) to go from derivatives with respect to $\partial\theta$ to derivatives with respect to ∂R in (26) and (27). Having performed this operation, we multiply equation (26) by $tan\,\theta$ and add it to equation (27). Keeping in mind that expression (52), as well as its first and second derivatives, in the area of boundary layer are approximately equal to zero, we arrive at the following equation:

$$\rho\left(\frac{v_\theta}{R}(v_R - v_\theta\, tan\,\theta)\right) = 2\cot 2\theta\frac{\partial P}{\partial R} - \mu\left(\frac{2v_R}{R^2}tan\,\theta + \frac{2\cot\theta}{R}\frac{\partial}{\partial R}(v_R - v_\theta\, tan\,\theta) + \frac{v_\theta\cos 2\theta}{(R\cos\theta)^2}\right); \quad (56)$$

Performing integration (56) and taking into account the following approximate equalities ($\alpha \approx 1$ in the area of boundary layer)

$$\int R\log R\,dR \approx 0; \quad (57)$$

$$\int R^{5\alpha-4}\log R\,dR \approx 0; \quad (58)$$

we arrive at the final formula for in-plane pressure for a sharp cone:

$$P = \frac{1}{2\cot 2\theta}\left(\left(\rho v_\theta \log\frac{R}{C} + \mu\left(\frac{2\cot\theta}{R} - \frac{1}{\sin\theta\cos\theta}\left(\frac{1}{R} - \left(\log\frac{R}{C}\right)\frac{\partial}{\partial R}\right)\right)\right)(v_R - v_\theta\, tan\,\theta) - \frac{\mu}{\sin\theta\cos\theta}\left(\frac{1}{R} - \left(\log\frac{R}{C}\right)\frac{\partial}{\partial R}\right)v_R\right). \quad (59)$$

In the Figs. 6 and 7 below the graphs for pressure corresponding to (59) are shown (when constructing graphs, we must substitute expression (54) into (59)).

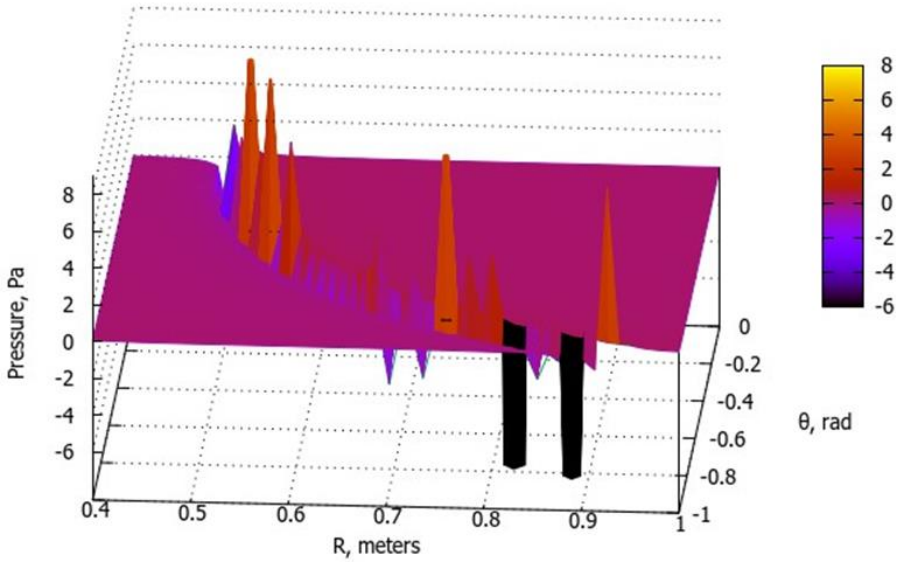

Figure-6. Graph for P in (59) at $\psi = 10°$ ($\theta_w = 80°$ ($1.4\,rad$)) and $A_0 = 200\ \frac{m}{sec}$.

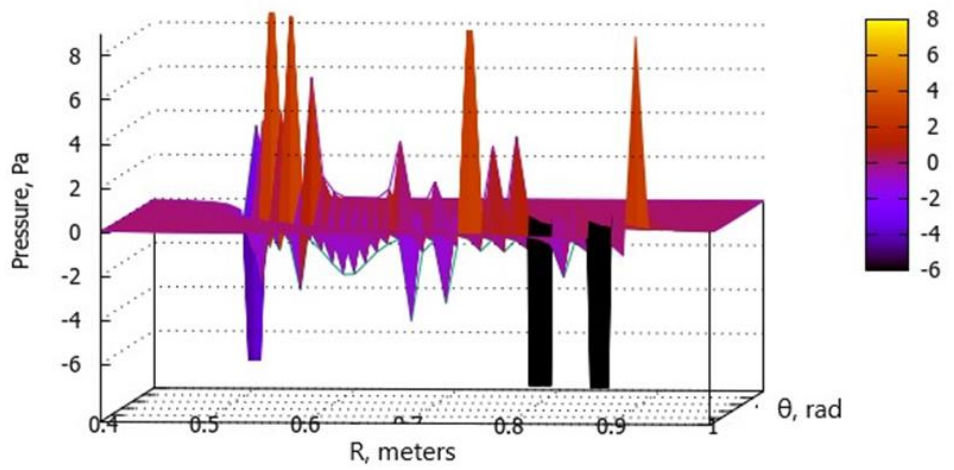

Figure-7. Graph for P in (59) at $\psi = 10°$ ($\theta_w = 80°$ ($1.4\ rad$)) and $A_0 = 200\ \frac{m}{sec}$ (another view).

Analyzing the graphs in Figs. 6 and 7 we must take into account that they should be shifted upward along the θ axis by 1.4 rad. After this, the point $R \approx 0.5\ m$ lying on the wall of the cone will correspond to the angle $\theta = 1.4\ rad$, which corresponds to movement in the plane (54) (Fig. 1a). This means that formula (59) requires additional debugging. Also, it should be remembered that these graphs are accurate only in the area of boundary layer ($\theta \approx 1.4$); and the pressure P in (59) is a difference between actual pressure in some point and hydrostatic pressure in the same point, therefore it can take negative values.

In addition to the constants (47) – (49) when constructing graphs, we also used the following:

$$\rho = 1\ \frac{kg}{m^3};\ \text{(density of air at } T \approx 300\ K, p \approx 10^5 Pa) \tag{60}$$

$$\mu = 0.00001\ Pa \cdot sec; \tag{61}$$

$$C = 10\ m. \tag{62}$$

4.2 Broad cone

4.2.1 Finding velocity components

Using first equalities in (9) and (10) and condition (24) for broad cone ($(uw)x = -(vw)y$) we find first derivatives of functions *(uw)* and *(vw)* by *∂x* and *∂y*:

$$\frac{\partial(uw)}{\partial x} = -(uw)\left(\frac{x}{x^2+y^2} + \frac{x}{y^2} - \frac{1}{x}\right); \tag{63}$$

$$\frac{\partial(vw)}{\partial x} = -(vw)\left(\frac{x}{x^2+y^2} + \frac{x}{y^2} - \frac{2}{x}\right); \tag{64}$$

$$\frac{\partial(uw)}{\partial y} = -(uw)\left(\frac{y}{x^2+y^2} + \frac{y}{x^2} - \frac{2}{y}\right); \tag{65}$$

$$\frac{\partial(vw)}{\partial y} = -(vw)\left(\frac{y}{x^2+y^2} + \frac{y}{x^2} - \frac{1}{y}\right); \tag{66}$$

Separately, we will focus on how to apply relation (11), which is the essence of the main theorem of tunnel mathematics, and thereby obtain derivatives of the indicated functions with respect to *∂z*.

First we apply the planar Laplacian operation to relation (11):

$$\Delta\left(\frac{1}{x}\cdot\frac{\partial(uw)}{\partial x}+\frac{1}{y}\cdot\frac{\partial(vw)}{\partial x}\right)=-\frac{\partial\Delta u}{\partial z}-\Delta\left(\frac{1}{\sqrt{x^2+y^2}}\cdot\frac{\partial(vw)}{\partial z}\right). \tag{67}$$

After this, using the harmonicity of function *u* (2), and the relations of tunnel mathematics for planar Laplacians (4) and (5), we obtain the required derivatives with respect to *∂z*:

$$\frac{\partial(uw)}{\partial z}=-(uw)\frac{xy\sqrt{x^2+y^2}}{\beta_3}\left(-\beta_2+\frac{x^2+y^2}{(uw)}\left(C_r+\frac{y}{x}C_i\right)\right); \tag{68}$$

where

$$\beta_2=-\left(\frac{x^2}{y^2}+\left(1+\frac{x^2}{y^2}\right)\left(2+\frac{x^2}{y^2}\right)\right)+\frac{2x^2}{x^2+y^2}+\frac{12(xy)^2}{(x^2+y^2)^2}; \tag{69}$$

$$\beta_3=(x^2+y^2)^2-x^2\left(4(x^2+y^2)-x^2\left(8-\frac{7x^2}{x^2+y^2}\right)\right)-(xy)^3\left(\frac{(y^2-x^2)}{xy}\frac{\partial C_r}{\partial z}-\frac{\partial C_i}{\partial z}\right)\frac{\partial z}{\partial(uw)}. \tag{70}$$

In order to simplify our calculations, we will set the following condition in (70):

$$\frac{(y^2-x^2)}{xy}\frac{\partial C_r}{\partial z}-\frac{\partial C_i}{\partial z}=0. \tag{71}$$

The easiest way to obtain an expression for $\frac{\partial(vw)}{\partial z}$ is to use (24) and (68):

$$\frac{\partial(vw)}{\partial z}=-(vw)\frac{xy\sqrt{x^2+y^2}}{\beta_3}\left(-\beta_2-\frac{x^2+y^2}{(vw)}\left(\frac{x}{y}C_r+C_i\right)\right); \tag{72}$$

Now using (63) – (66), (68) and (72) we get expressions for required functions *(uw)* and *(vw)*:

$$(uw)=B_0B_1\frac{xy^2}{x^2+y^2}\frac{b_1^2}{a_1a_2^2}\exp[1-\frac{1}{2}\left(\frac{x^2+y^2}{xy}\right)^2+zxy\sqrt{x^2+y^2}\frac{\beta_2}{\beta_3}-\frac{xy(x^2+y^2)^{3/2}}{\beta_3}\int\left(C_r+\frac{y}{x}C_i\right)\frac{dz}{(uw)}] \tag{73}$$

$$(vw)=B_0B_2\frac{x^2y}{x^2+y^2}\frac{b_1^2}{a_1^2a_2}\exp[1-\frac{1}{2}\left(\frac{x^2+y^2}{xy}\right)^2+zxy\sqrt{x^2+y^2}\frac{\beta_2}{\beta_3}+\frac{xy(x^2+y^2)^{3/2}}{\beta_3}\int\left(\frac{x}{y}C_r+C_i\right)\frac{dz}{(vw)}] \tag{74}$$

where $B_0, B_1, B_2, a_1, a_2, b_1$ are the constants; $[B_0]=[B_1]=[B_2]=\frac{m}{sec}$; $[a_1]=[a_2]=[b_1]=m$.

Using obtained results, we can construct the components of the vector velocity field in Cartesian coordinate system. In order to satisfy (24) ($(uw)x=-(vw)y$) we select from (73) and (74) the components of analytical functions [7] in following manner:

$$u=-B_1\frac{y}{a_2}e^{-z/b_2}; \tag{75}$$

$$v=B_2\frac{x}{a_1}e^{-z/b_2}; \tag{76}$$

where b_2 is a constant.

It is easy seen that (2) and (3) are satisfied automatically. Besides, in (75) and (76) the following equalities for constants hold:

$$B_1 = B_2;\ a_1 = a_2. \tag{77}$$

We also allowed the following equalities in (73) and (74):

$$-\frac{xy(x^2+y^2)^{3/2}}{\beta_3}\int\left(C_r+\frac{y}{x}C_i\right)\frac{dz}{(uw)} = \frac{xy(x^2+y^2)^{3/2}}{\beta_3}\int\left(\frac{x}{y}C_r+C_i\right)\frac{dz}{(vw)} = e^{-z/b_2}. \tag{78}$$

We did this in order to simplify our calculations and avoid encountering integral equations at this stage of research. In addition, it should be remembered that we can assign any functions, depending on *z*, to the constants C_r and C_i.

Now we obtain from (73) and (74) such relation for *w*:

$$w = B_0\frac{xy}{x^2+y^2}\frac{b_1^2}{a_1^2}\exp\left[1-\frac{1}{2}\left(\frac{x^2+y^2}{xy}\right)^2+\ zxy\sqrt{x^2+y^2}\frac{\beta_2}{\beta_3}\right]; \tag{79}$$

where we assume the following equality for the constants:

$$b_1^2 = 2a_1^2; \tag{80}$$

Using (15) – (17) and (18) – (20) we can obtain the components of the vector velocity field in modified (8) spherical coordinate system:

$$v_R = 2B_0B_3\sin\theta\exp\left[1-\frac{1}{2}B_3^{-2}+\ B_3B_6\,tan\,\theta\right]; \tag{81}$$

$$v_\theta = 2B_0B_3\cos\theta\exp\left[1-\frac{1}{2}B_3^{-2}+\ B_3B_6\,tan\,\theta\right]; \tag{82}$$

where the constants are assigned the following expressions:

$$B_3 = \frac{\sin 2\varphi}{2}; \tag{83}$$

$$B_6 = \frac{-B_4+2B_5(1+6(1-B_5))}{1-B_5(4-B_5(8-7B_5))}; \tag{84}$$

$$B_4 = \cot^2\varphi + (1+\cot^2\varphi)(2+\cot^2\varphi); \tag{85}$$

$$B_5 = \cos^2\varphi. \tag{86}$$

It is seen from (81) and (82) that components v_R and v_θ don`t depend on *R*. This is consequence of condition (71) for β_3.

$$v_\varphi = \Omega R\cos\theta\exp\left[\frac{R}{b_2}(\sin\theta_w-\sin\theta)\right]; \tag{87}$$

where Ω is the angular velocity, $[\Omega] = rad/sec$; θ_w is the angle corresponding to the wall of cone; for a broad cone (Fig. 1b) we assume that $\theta_w = 10° = 0.174\ rad$ ($\psi = 80°$).

Below in Figs. 8 – 10 we show graphs of the components of the vector velocity field in (81), (82) and (87).

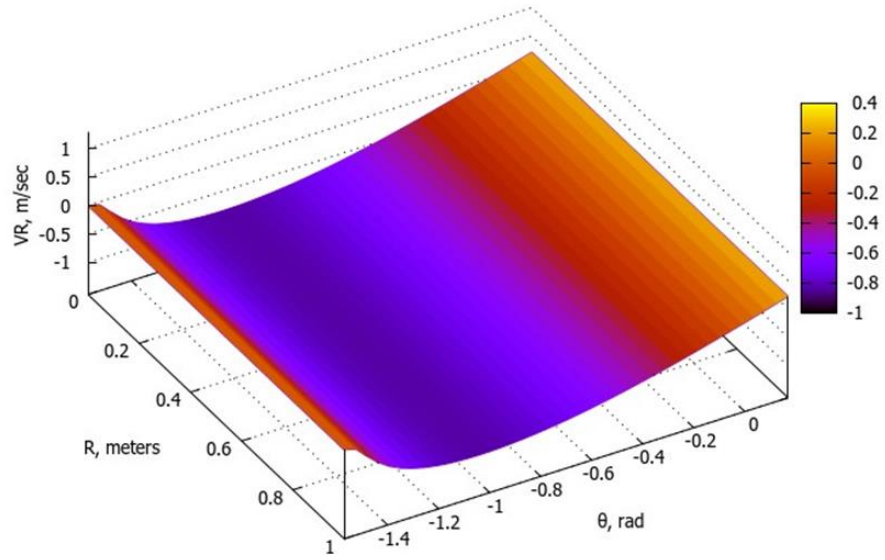

Figure-8. Graph for v_R component in (81) at $\psi = 80°$ ($\theta_w = 10°$ ($0.174\ rad$)) and $B_0 = 200\ \frac{m}{sec}$.

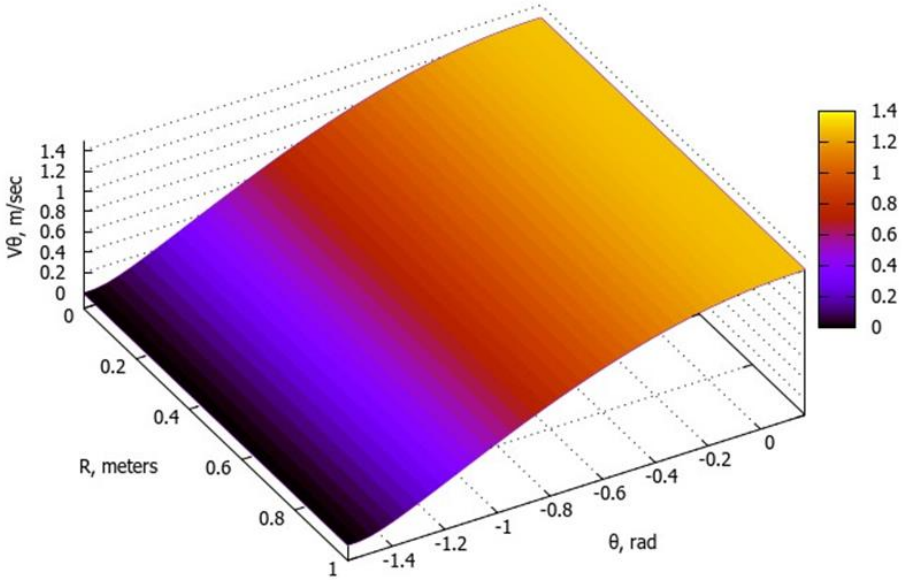

Figure-9. Graph for v_θ component in (82) at $\psi = 80°$ ($\theta_w = 10°$ ($0.174\ rad$)) and $B_0 = 200\ \frac{m}{sec}$.

When constructing graphs, we assume the values of the remaining constants as follows:

$B_3 = 0.3$; (88)

$B_6 = 0.5$. (89)

As can be seen from Figs 8 and 9, the simplifications we made lead to the impossibility of meeting the non-slip boundary conditions for a broad cone (especially, for v_θ component). However, as we will see below, this situation will not affect the fulfillment of similar conditions for a rotating disk.

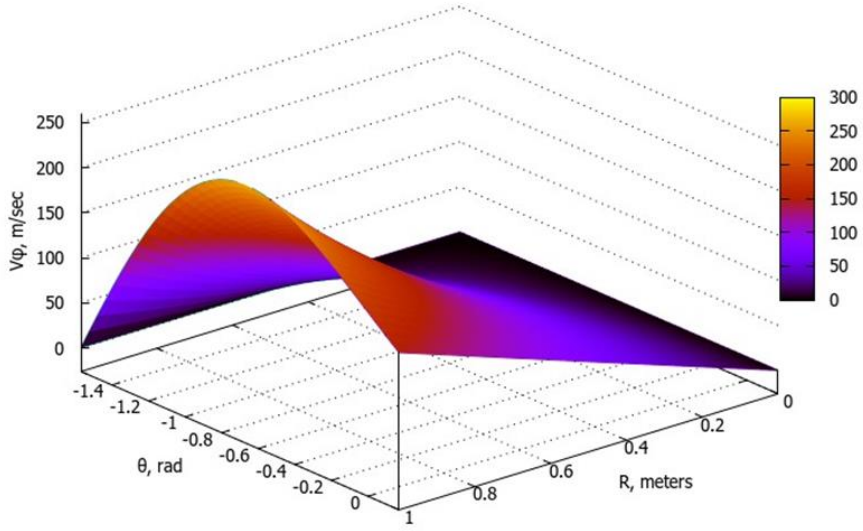

Figure-10. Graph for v_φ component in (87) at $\psi = 80°$ ($\theta_w = 10°$ ($0.174\ rad$)); $\Omega = 150\ \frac{rad}{sec}$ and $b_2 = 1\ m$.

4.2.2 Finding pressure

First we check the equation of continuity for incompressible case. Substituting (81) and (82) in (29), we obtain such expression:

$$\frac{\partial v_R}{\partial R} + \frac{2v_R}{R} + \frac{\partial v_\theta}{R\partial\theta} - \frac{v_\theta \tan\theta}{R} = \frac{B_3 B_6}{\cos^2\theta}\frac{v_\theta}{R}; \tag{90}$$

It is seen that the expression (90) does not exceed the values of v_θ.

Translating equations (26) and (27) into the plane

$$z = R\sin\theta = 0.1 \tag{91}$$

and, taking advantage of the fact that the expressions (81) and (82) do not depend on R, we arrive at the following fairly simple equations:

$$-\rho\frac{v_\varphi^2}{R} = -\frac{\partial P}{\partial R}; \tag{92}$$

$$\rho\frac{v_\varphi^2 \tan\theta}{R} = \frac{\partial P}{\partial R}\cot\theta - \mu\frac{v_\theta}{(R\cos\theta)^2}; \tag{93}$$

When deriving equations (92) and (93), we also took into account the conditions for our model of broad cone: $v_R, v_\theta \ll v_\varphi$ (large centrifugal flows).

Now we multiply equation (93) by $\tan\theta$ and subtract equation (92) from it, after which we find the expression for the pressure in the plane (91):

$$P = \frac{1}{2}\left(\rho\Omega^2\frac{b_2}{2(\sin\theta_w - \sin\theta)}\exp\left[\frac{2R}{b_2}(\sin\theta_w - \sin\theta)\right]\left(R - \frac{b_2}{2(\sin\theta_w - \sin\theta)}\right) - \mu\frac{v_R}{R\cos^2\theta}\right); \tag{94}$$

where the expression for v_R in is taken from (81).

Below in Fig. 11 we show graph of the pressure in (94):

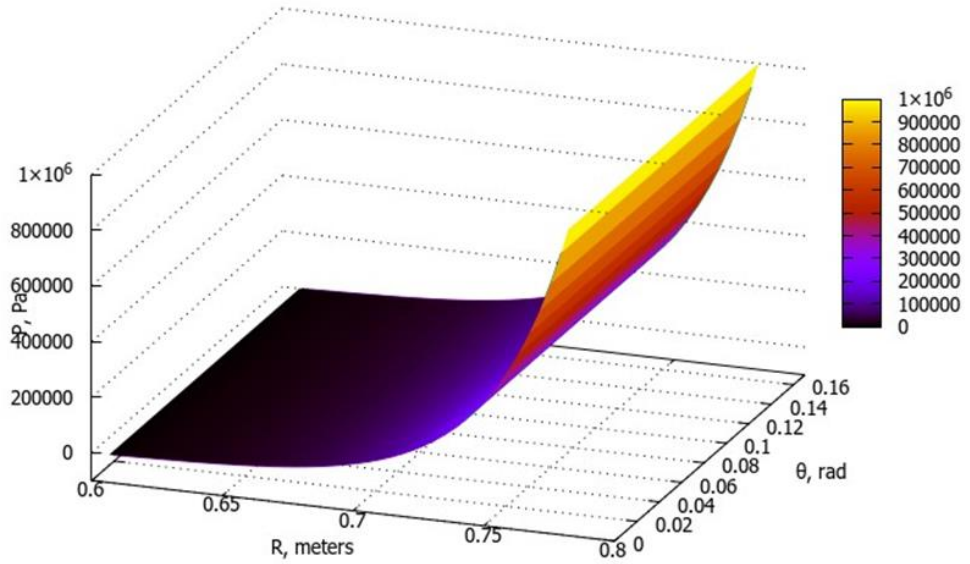

Figure-11. Graph for P in (94) at $\psi = 80°$ ($\theta_w = 10°$ ($0.174\ rad$)); $\Omega = 150\ \frac{rad}{sec}$ and $b_2 = 0.01\ m$.

When constructing graph, we assume the values of the remaining constants as follows:

$$B_3 = -0.3; \tag{95}$$

$$B_6 = 0.5. \tag{96}$$

Values for ρ and μ correspond to (60) and (61).

It is seen from Fig. 11 that, unlike a sharp cone (Figs. 6 and 7), the pressure around a broad cone in a plane (91) increases smoothly and does not have sharp peaks.

We can also use equation (28), which does not contain pressure due to the axial symmetry of the flow, to obtain a valuable relation characterizing the liquid or gas around a rotating broad cone. Substituting expressions (81), (82) and (87) into equation (28) we obtain the following equality:

$$-\rho w(1 - \sin\theta \sin\theta_w) = \mu\left(\frac{4\sin\theta_w}{R} + \frac{(\sin\theta_w - \sin\theta)^2}{b_2}\right); \tag{97}$$

where the expression for w in is taken from (79).

Relation (97) connects the density and viscosity of a liquid or gas around a rotating broad cone and is satisfied throughout the entire volume of the flow. This relation can be used to determine calibration coefficients b_2, B_3, B_6.

4.3 Disk

4.3.1 Finding velocity components

We get solution for a rotating disk as a limit transition for a broad cone (Fig. 1). To achieve this goal, we must introduce the following obvious transformations into the broad cone solutions (which is equivalent to passing to cylindrical coordinates):

$$\theta_w \to 0; \tag{98}$$

$$\theta \to -\theta; \tag{99}$$

$$v_R \to v_R; \tag{100}$$

$$v_\theta \to v_{-\theta}; \tag{101}$$

$$v_\varphi \to v_\varphi; \tag{102}$$

$$R\cos\theta \to r; \tag{103}$$

$$-\mathrm{R}\sin\theta \to -z; \tag{104}$$

$$R^2 = r^2 + (-z)^2 = r^2 + z^2; \tag{105}$$

$$v_r = v_R\cos\theta + v_{-\theta}\sin\theta\,; \tag{106}$$

$$-v_z = -v_R\sin\theta + v_{-\theta}\cos\theta\,; \tag{107}$$

Substituting relations (81) and (82) for a broad cone into relations (106) and (107) for a disk we obtain expressions for v_r and $-v_z$ components of the fluid vector velocity field for a rotating disk in cylindrical system of coordinates:

$$v_r = 2B_0B_3\frac{rz}{r^2+z^2}\exp\left[1-\frac{1}{2}B_3^{-2}+\ B_3B_6\frac{z}{r}\right]\left(1+\exp\left[-2\ B_3B_6\frac{z}{r}\right]\right); \tag{108}$$

$$-v_z = -2B_0B_3\frac{z^2}{r^2+z^2}\exp\left[1-\frac{1}{2}B_3^{-2}+\ B_3B_6\frac{z}{r}\right]\left(1-\left(\frac{r}{z}\right)^2\exp\left[-2\ B_3B_6\frac{z}{r}\right]\right); \tag{109}$$

Substituting relations (98) and (103) into (87) we obtain expressions for v_φ component:

$$v_\varphi = \Omega r e^{-z/b_2}; \tag{110}$$

Below in Figs. 12 – 15 we show graphs of the components of the vector velocity field in (108) – (110).

When constructing graphs in Figs. 12 – 15, we assume the values of the remaining constants as follows:

$$B_3 = \begin{cases} 0.3\ for\ v_r\ component; \\ -0.3\ for\ -v_z\ component; \end{cases} \tag{111}$$

$$B_6 = 0.5. \tag{112}$$

It is seen from Figs. 12 – 15 that the non-slip boundary conditions for a rotating disk are fulfilled.

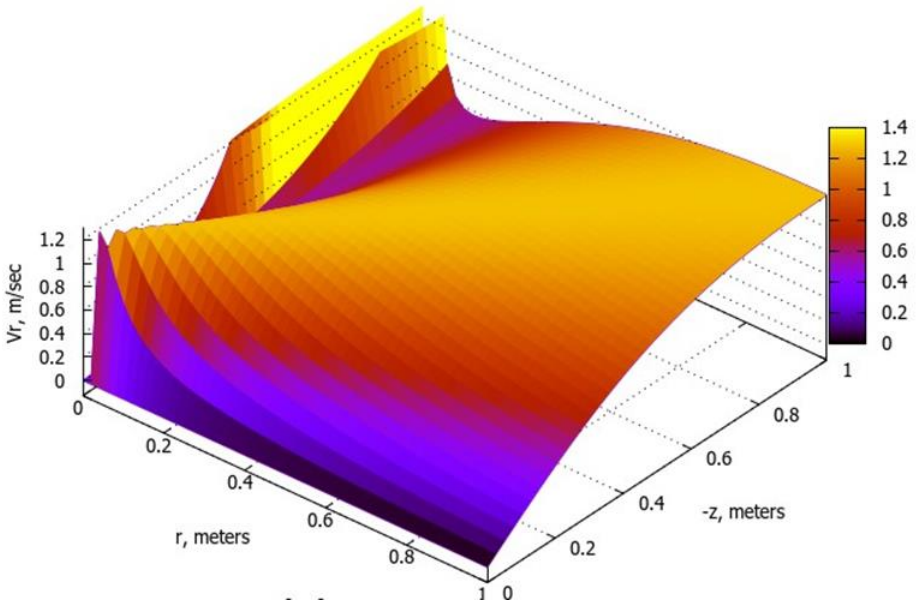

Figure-12. Graph for v_r component of the fluid vector velocity field for a rotating disk in (108) at $B_0 = 200\ \frac{m}{sec}$.

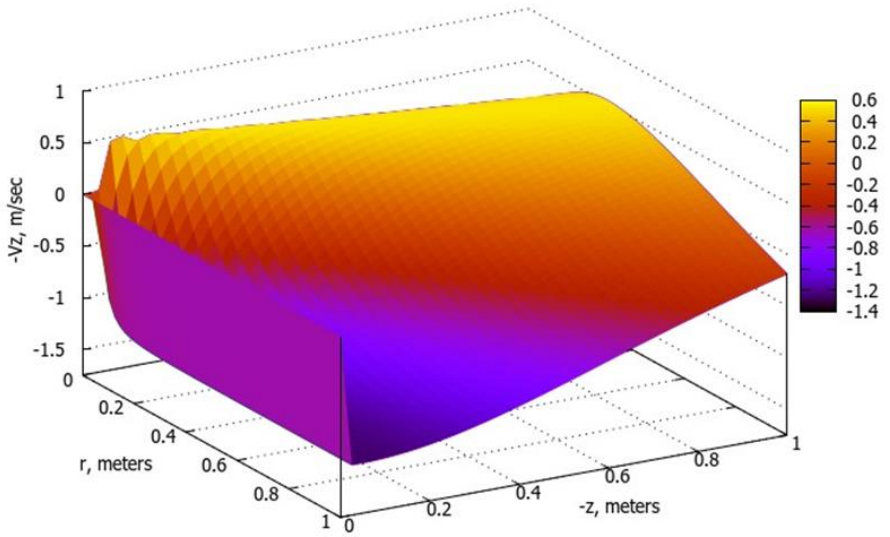

Figure-13. Graph for $-v_z$ component of the fluid vector velocity field for a rotating disk in (109) at $B_0 = 200\ \frac{m}{sec}$.

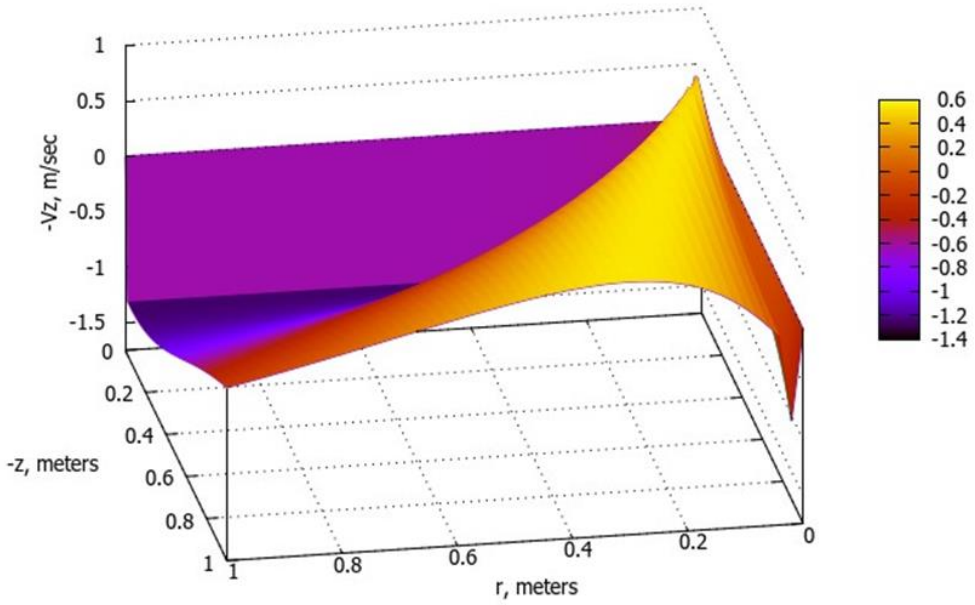

Figure-14. Graph for $-v_z$ component of the fluid vector velocity field for a rotating disk in (109) at $B_0 = 200\ \frac{m}{sec}$ (another view).

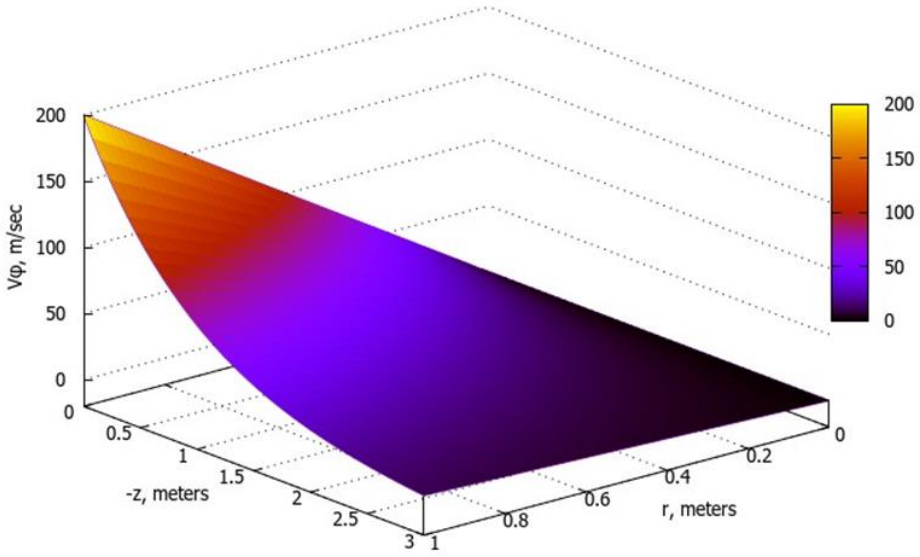

Figure-15. Graph for v_φ component of the fluid vector velocity field for a rotating disk in (110) at $\Omega = 200\ \frac{rad}{sec}$ and $b_2 = 1\ m$.

If our solutions are similar to the famous Karman`s solutions for laminar flow entrained by a rotating disk, then we will consider our theory to be somewhat successful. Below in Fig. 16 Karman's solution is given.

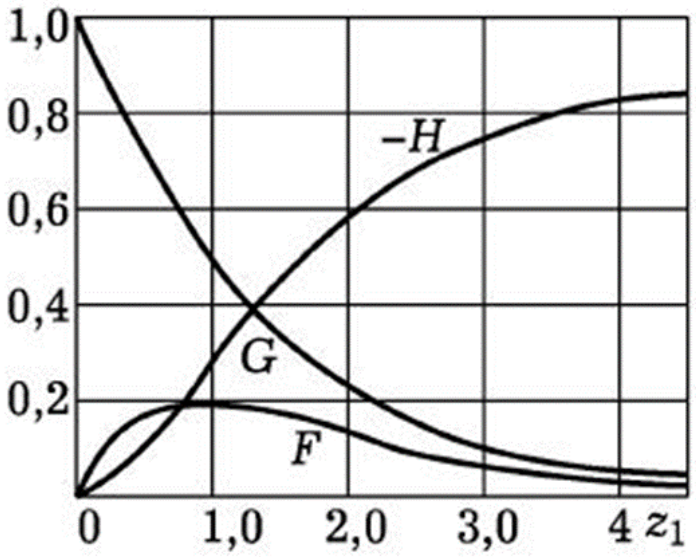

Figure-16. Solution to the problem for an infinite rotating disk using numerical methods in [1]. The function *F* corresponds to the radial velocity v_r, the function *G* to the azimuthal velocity v_φ and the function *H* to the axial velocity v_z (here it is assumed that the z-axis is directed upward, in contrast to our Fig.1).

Functions in Fig. 16 are the numerical solutions to the following system of ordinary differential equations, to which the Navier-Stokes equations were reduced:

$$F^2 - G^2 + F'H = F''; \quad (113)$$

$$2FG + G'H = G''; \quad (114)$$

$$HH' = P' + H''; \quad (115)$$

$$2F + H' = 0; \quad (116)$$

with such boundary conditions:

$$F = 0, G = 1, H = 0 \; at \; z_1 = 0; \quad (117)$$

$$F = 0, G = 0 \; at \; z_1 = \infty. \quad (118)$$

Comparing graphs in Figs. 12 – 15 (at $r = const$) with corresponding functions in Fig 16, we see that solutions for v_r and v_φ components obtained in tunnel mathematics space are similar to the Karman`s solutions. For the axial components $v_z$, significant differences are observed. To explain these discrepancies, we must remember that in the Karman`s model the disk is considered to be infinite, but we consider the disk to have a finite radius. For a disk of finite radius, the axial velocity at infinity never tends to any constant value; it rather tends to zero, remaining non-zero and directed towards the disk in a narrow funnel around the axis of the disk. It is precisely this picture of physical phenomena that corresponds to the solution for the axial component in Figs. 13 and 14.

4.3.2 Finding pressure

Using (98) – (105) we transform expression (94) for pressure into one that works for a rotating disk:

$$P = \frac{\rho\Omega^2 b_2}{4}\frac{(r^2+z^2)}{z}\exp\left[\frac{2z}{b_2}\right]\left(1-\frac{b_2}{2z}\right) - \mu B_0 B_3 \frac{(-z)}{r^2}\exp\left[1-\frac{1}{2}B_3^{-2} + B_3 B_6\frac{(-z)}{r}\right]. \quad (119)$$

Below in Fig. 17 we show graph of the pressure in (119) near the surface of the disk ($z = 0.001\ m$):

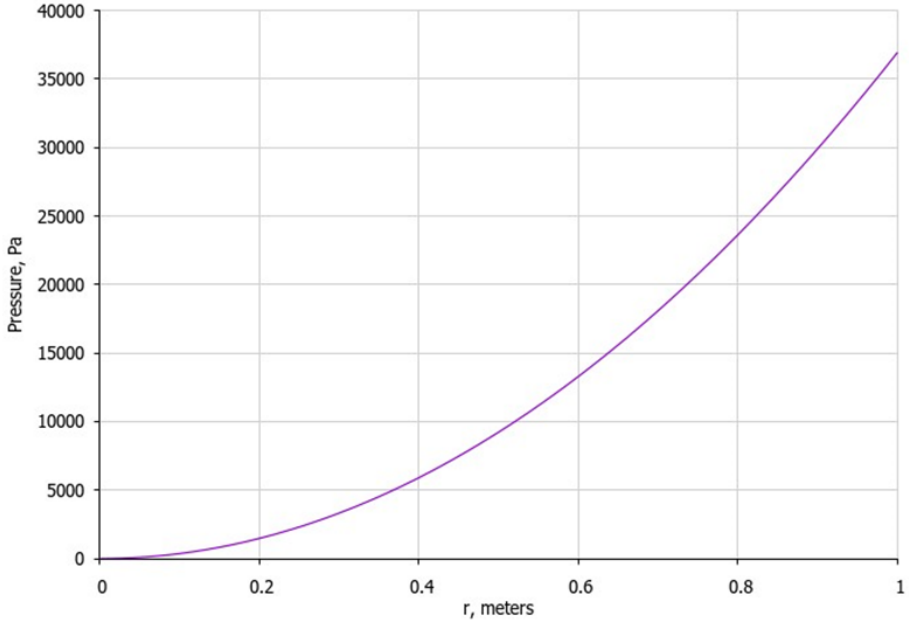

Figure-17. Graph for P in (119) at $\Omega = 200\ \frac{rad}{sec}$, $B_0 = 200\ \frac{m}{sec}$ and $b_2 = 0.001\ m$.

The remaining constants correspond to those established in (60), (61), (95) and (96).

Relation (97) for a rotating disk is as follows:

$$-\rho w' = \frac{\mu}{b_2}\frac{z^2}{(r^2+z^2)}; \quad (120)$$

where

$$w' = 2B_0 B_3 \exp\left[1-\frac{1}{2}B_3^{-2} + B_3 B_6\frac{z}{r}\right]. \quad (121)$$

5. Conclusion

We have partially succeeded in simulating the Karman`s solution for laminar flow entrained by a rotating disk. For the radial and azimuthal velocity components the coincidence is quite good. Significant differences are observed for the axial velocity component. This is due to the fact that the methods of tunnel mathematics are primarily aimed at obtaining solutions that correspond to the actually observed picture of physical phenomena; mathematical accuracy is relegated to the background. The resulting formulas for calculating the pressure in flows entrained by a sharp cone, a broad cone and a disk are quite simple and easy to use, but require experimental confirmation. Our model shows that for a sharp cone near the apex there is a step change in the velocity

components, reminiscent of quantization, due to which the flow near the apex of the sharp cone can be unstable. We believe that the methods of tunnel mathematics can be applied not only to the dynamics of liquids or gases, but in general to any area of physics where it is necessary to solve equations containing Laplacians.

6. References

[1] Landau and Lifshitz (1987). Fluid Mechanics, Course of Theoretical Physics, Volume 6, Second English Edition, Pergamon Press, pp. 75-77, 162, 315.
[2] Schlichting, Hermann (1979). Boundary-Layer Theory, 7th ed., McGraw Hill, New York, U.S.A, pp. 102-106, 647, 648.
[3] Štigler, J. Analytical Formula for the Mean Velocity Profile in a Pipe Derived on the Basis of a Spatial Polynomial Vorticity Distribution. Water 2021, 13, 1372; https://doi.org/10.3390/w13101372
[4] Zhao, B., Tang, W., Lin, P., and Wang, Q. (January 4, 2023). On the Unsteady Rotationally Symmetric Flow Between a Stationary and a Finite Rotating Disk With a Given Change in the Axial Velocity. ASME. J. Fluids Eng. April 2023; 145(4): 041301; https://doi.org/10.1115/1.4056415
[5] Biruk Alemayehu Petros. (April 6, 2024). Simplification of the Navier-Stokes Equations for Incompressible Fluids via Local Linearization of Variable Functions. Preprint.
[6] P. Henrik Alfredsson, Kentaro Kato, and R. J. Lingwood. (January 2024). Flows Over Rotating Disks and Cones. Annu. Rev. Fluid Mech. 2024. 56:45–68; https://doi.org/10.1146/annurev-fluid-121021-043651
[7] Lavrentiev M. (1972). Méthodes de la théorie des fonctions d'une variable complexe. / M. Lavrentiev, B. Chabat: traduit du russe. — Moscou: Mir, — 728 p.
[8] Patil, Dinkar and Dighe, Snehal V. and Khand, Dipali S., Recent Developments in Integral Transforms (December 26, 2023). IJRAR December 2023, Volume 10, Issue 4, Available at SSRN: https://ssrn.com/abstract=4675990
[9] Shams A. Ahmed, Rania Saadeh, Ahmad Qazza, Tarig M. Elzaki. (2024). Applying Conformable Double Sumudu – Elzaki Approach to Solve Nonlinear Fractional Problems. Progr. Fract. Differ. Appl. 10, No. 2, 271-286; doi:10.18576/pfda/100208
[10] Igor V. Shevchuk. (2022). An asymptotic expansion method vs a self-similar solution for convective heat transfer in rotating cone-disk systems. Physics of Fluids 34, 103610; https://doi.org/10.1063/5.0120922
[11] Oleh G. Shvydkyi. (2022). Tensor foundations of tunnel mathematics, Preprint, https://doi.org/10.21203/rs.3.rs-2827573/v1
[12] Oleh G. Shvydkyi. (2024). Analytical Solution to the Steady Navier-Stokes Equation for a Supersonic Cone in the Area of Boundary Layer Behind the Shock Wave by Means Tunnel Mathematics. Acceleron Aerospace Journal, 2(6), 346–367. https://doi.org/10.61359/11.2106-2429.
[13] Taofiq O. Amoloye. (2024). Modeling the unsteady wake of an impulsively started circular cylinder using refined potential flow theory, Phys. Scr. 99 085207. https://doi.org/10.1088/1402-4896/ad4ace
[14] Kentaro KATO, Rebecca J. LINGWOOD, P. Henrik ALFREDSSON (2023). Rotating disks and cones a centennial of von Kármán's 1921 paper. Journal of Fluid Science and Technology. Volume 18 Issue 1 Pages JFST0003; https://doi.org/10.1299/jfst.2023jfst0003
[15] Koji Ohkitani (2023). Numerical comparison of two-dimensional Navier-Stokes flows on the whole plane and the periodic domain. Phys. Rev. Fluids 8, 124607; https://doi.org/10.1103/PhysRevFluids.8.124607

7. Conflict of Interest

The author declares no competing conflict of interest.

8. Funding

No funding was received to support this study.